Available online at www.sciencedirect.com
SCIENCE DIRECT®
Journal of Solid State Chemistry 172 (2003) 319–326
JOURNAL OF SOLID STATE CHEMISTRY
http://elsevier.com/locate/jssc

The composite structure of $Cu_{2.33-x}V_4O_{11}$

Patrick Rozier[a,*] and Sven Lidin[b]

[a] Centre d'Elaboration de Matériaux et d'Etudes Structurales/CNRS, BP 4347, 31055 Toulouse Cedex 4, France
[b] Arrhenius Laboratory, Department of Inorganic Chemistry, Stockholm University, S-106 91 Stockholm, Sweden

Received 24 June 2002; received in revised form 29 August 2002; accepted 3 September 2002

Abstract

The copper vanadium oxide bronze $Cu_{2.33-x}V_4O_{11}$ exhibits a three part composite structure refined on the basis of XRD low-temperature studies. It crystallizes in the triclinic system with the non-centric superspace group *X1* and cell parameters $a = 15.280(3)$ Å; $b_1 = 3.616(1)$ Å; $c = 14.674(3)$ Å; $\alpha = 90.0°$; $\beta = 101.95(3)°$; $\gamma = 90.0°$ with a modulation q-vector equal to (0,0.11,0). The three different parts of this composite structure differ by their *b*-unit cell repeat defined as b_1 ; $b_2 = 2.964(1)$ Å ($b_2^* = b_1^* + 2q$) and $b_3 = 3.257(1)$ Å ($b_3^* = b_1^* + 1q$). These parts are respectively associated to the V_4O_{11} substructure and to each of the two different copper sites. Such refinement allows us to describe the structure using only one and fully occupied crystallographic site for each of the Cu ions. The maximum composition ($x = 0$) is then achieved. Bond valence sum calculations on the basis of such composite structure is in agreement with electronic structure calculation made using the average one and allows us to attribute the proper valence state to each Cu ions. Then, the calculated ratio appears, contrary to the average structure, in prefect agreement with the one deduced from XPS experiment.

Keywords: Copper vanadium oxide; Composite structure; Superstructure

1. Introduction

The $M_xV_2O_5$ vanadium oxide bronzes (VOBs) represent an extensive family of phases with original crystal structures and a wide variety of chemical or physical properties intimately associated with the variable stoichiometry of the *M* elements (alkali, alkaline earth, Cu, Ag, Zn) and the mixed valence of the vanadium (V^{5+}–V^{4+}). Among these VOBs the copper vanadium bronze family appears to be special mainly due to the possibility of combining both Cu^{+}–Cu^{2+} and V^{5+}–V^{4+} valence states. One interesting compound was first isolated by Galy et al. [1] and formulated as $Cu_xV_4O_{11}$ (*Cm*, $a = 15.38$ Å, $b = 3.61$ Å, $c = 7.37$ Å, $\beta \sim 102°$). In 1992, Saito et al. [2] studying this phase in a wide compositional range observed the existence of a charge transfer between the Cu and V cations. They reported a magnetic and structural transition at $T_c \cong 300$ K and a possible incommensurate cell. More recently (1996) Kato et al. [3] reported an incommensurately modulated ($\boldsymbol{q_1} = 0.23\mathbf{b}^*$) structure determination of $Cu_{2.12}V_4O_{11}$ surprisingly related to only one kind of copper site, the other one appearing to be randomly occupied.

Both interesting physical properties as well ambiguities about the crystal-chemistry of this phase prompted further solid-state chemical investigations. The Bragg and Weissenberg diagrams confirmed the existence of an incommensurate modulation. Based on single-crystal XRD, a detailed description of the average structure (Fig. 1) allowed us to show that the Cu ions exhibit unusual coordination. Moreover, on the basis of the examination of the different copper sites localization we determined the maximal occupation on each site as well as their distribution driving to reformulate this phase as $Cu_{2.33-x}V_4O_{11}$ in order to underline the maximal occupancy, i.e. the highest copper content reached when $x = 0$ [4].

A temperature-dependent electron diffraction study has been made. In addition to the results of Kato et al. [3], evidence was thereby found (at low temperature) for two distinct and mutually independent incommensurate modulations ($\mathbf{q}_2 = 1/2\mathbf{c}^* + \sim 0.12\mathbf{b}^*$); ($\mathbf{q}_3 = \pm 1/2\mathbf{a}^* + \sim 0.16\mathbf{b}^*$), the last one giving very weak set of satellites [5]. These modulations are expected to be associated with the three-dimensional ordering of Cu ions, the two

*Corresponding author. Fax: +33-5-6225-7999.
E-mail address: rozier@cemes.fr (P. Rozier).

0022-4596/03/$ - see front matter © 2003 Elsevier Science (USA). All rights reserved.
doi:10.1016/S0022-4596(02)00066-X

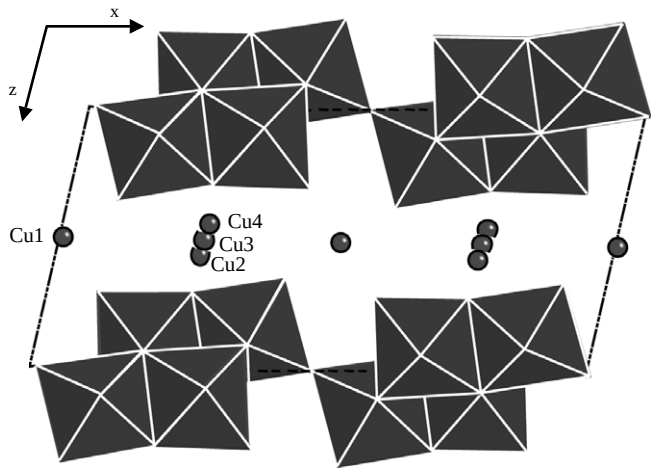

Fig. 1. Projection of the $Cu_{2.33-x}V_4O_{11}$ structure.

distinct channel types which run along **b** between the V_4O_{11} layers of the average structure.

The aim of this paper is then to report the determination, based on single-crystal X-ray diffraction data, of this incommensurately modulated structure in order to specify the origin of the modulation as well as the associated structural relaxation.

2. Experimental

2.1. Synthesis

CuO, V_2O_5 (Aldrich 99.99%) and V_2O_4 oxides were used as starting materials. V_2O_4 was obtained by heating a stoichiometric mixture of V_2O_3 and V_2O_5 under vacuum for 12 h, whereas V_2O_3 was obtained by a treatment of pure V_2O_5 under hydrogen flux.

The mixture of stoichiometric amounts of starting oxides, after grinding, was sealed in a quartz ampoule under vacuum and heated up to 600°C for 12 h. To obtain well-crystallized samples, re-heating was performed under the same conditions. The different products were checked by X-ray diffraction.

2.2. Crystal growth

As V^{4+}-based oxides were used, the crystals were prepared under vacuum. Single crystals were obtained using a direct melting and slow cooling method, or via chemical transport reaction, the transporting agent being here the selenium dioxide, (SeO_2). In the latter way, 10% SeO_2 (by weight) was mixed with $Cu_{2.33}V_4O_{11}$ powder. This mixture was sealed in a quartz ampoule under vacuum, heated up to 600°C for 1 hour, slowly cooled down to 450°C and then quenched down to room temperature. In both cases, a mixture of single crystals with a needle or platelet shape was obtained. Some of these were selected for complete X-ray single-crystal analysis. The rest of the sample was crushed to obtain a fine powder suitable for powder XRD analysis. The latter experiment allowed us to confirm the sample to be a single-phase material.

2.3. Crystallographic study

2.3.1. XRD Powder data

The XRPD data were obtained using a Seifert XRD 3000 TT diffractometer with monochromatized Cu$K\alpha$ radiation ($\lambda = 1.5418$ Å). X-ray profiles are measured in the θ range $2^\circ \leqslant \theta \leqslant 40^\circ$ in a step scan mode with a counting time of 10 s and an angular step of 0.01° in θ.

2.3.2. Single crystal XRD

X-ray experiments were carried out on a STOE IPDS diffractometer equipped with a sealed tube (Mo$K\alpha$) X-ray source and an Oxford-Cryo-stream cooling device. The measurement was done with 0.5° φ scans in the range $0^\circ < \varphi < 200^\circ$. Data reduction were carried out using the software X-shape and X-red [6], while the refinement was done using JANA2000 [7] and proceeded quite smoothly for the first composite part. A preliminary investigation at ambient temperature established the crystal quality. Further, these data were used to refine the modulated structure of the first copper site (Cu1).

3. Results and discussion

3.1. Structure refinement

As described in previous papers, the incommensurate modulation of the compound $Cu_{2.33}V_4O_{11}$ shows a rather complex temperature dependence. The basic monoclinic cell is C-centered and has the parameters

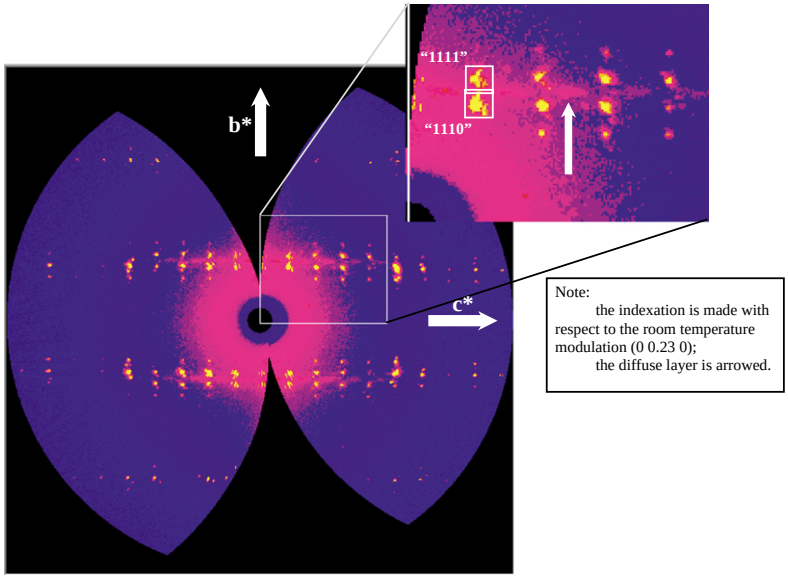

(a)

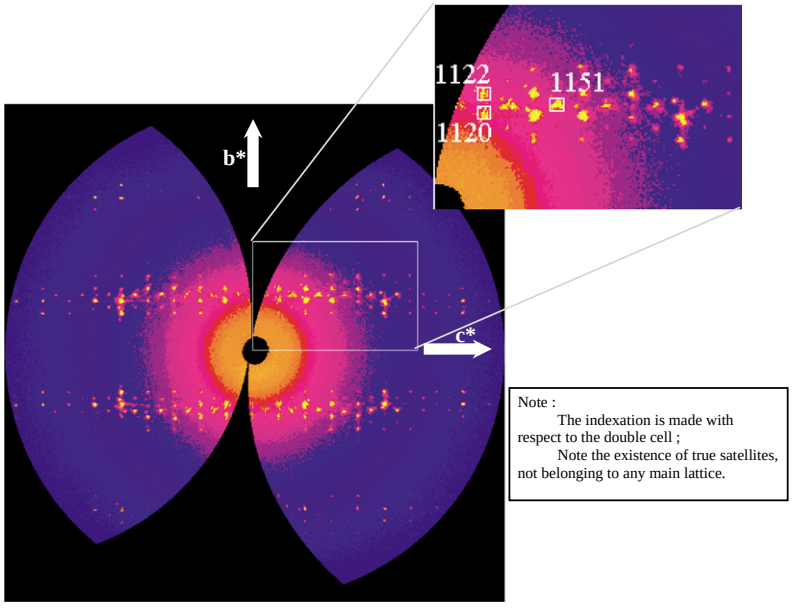

(b)

Fig. 2. Reciprocal lattice sections extracted perpendicular to **a** from the raw data: (a) measurement at ambient temperature; (b) measurement at 110 K.

$a = 15.28$ Å, $b = 3.62$ Å, $c = 7.34$ Å, and $\beta = 101.95°$. At ambient conditions, the modulation vector is parallel to $\mathbf{b}^*$ with the approximate magnitude $\mathbf{q} = (0, 0.23, 0)$ as given by Kato et al. [3]. It has been shown by Withers et al. [5] that at 110 K two additional phenomena are observed; a second set of satellites occur at $(00\ 1/2) + q/2$, and a third, very weak, set occurs at $(1/2, \sim 0.16, 0)$. Fig. 2 shows sections of reciprocal space extracted, using SPACE [8], from the raw data for the room temperature (a) and the 110 K structure (b). The diffuse layer perpendicular to $\mathbf{b}^*$-axis observed at the room temperature is in agreement with TEM experiments. It condenses out, at 110 K, into well-defined Bragg reflections traducing the second modulation. However, even if the low-temperature single-crystal X-ray experiment shows that the second set of satellites has measurable intensities, the weak third set is not discernable.

The diffraction data are then consistent with a (3 + 1)-dimensional, centered, monoclinic cell $a = 15.280(3)\mathring{A}$, $b = 3.616(1)$Å, $c = 14.674(4)$Å, $\beta = 101.95(3)°$, $\mathbf{q_1} \approx 0.11(1)\mathbf{b}^*$. Note that the **c**-axis has been doubled to take into account the commensurate superstructure (00 1/2). The centering vectors are 0000; 1/2 1/200; 001/2 1/2 and the combination 1/2 1/2 1/2 1/2. Apart from the systematic extinctions associated with the centering conditions, there were no absences indicating translational

symmetries (glides or screws) and the refinement was therefore first performed in the non-centric group *Xm* (corresponding to the group *Cm* used for the room temperature structure), *X* indicating the non-standard centering.

As a starting model, the positional parameters from the room temperature refinement was used. The intensity distribution of the satellite reflections clearly indicate a composite behavior, and after several attempts it was found that the most attractive model is achieved using three composite parts; one for the vanadium oxide sub-structure and one each for the two independent copper positions that occur in tunnels defined by the first sub-structure. The second and third composite parts have the same ac-base plane structure, but they differ in their **b**-axis repeat. The position of Cu1 (linear and triangular surrounding), that is reasonably well ordered at room temperature even if three different crystallographic positions are necessary to describe it, is governed mainly by the room temperature modulation vector (0, 0.23, 0), i.e. $2\mathbf{q_1}$, while Cu2 (tetrahedral surrounding) that is quite disordered at ambient conditions (mainly evidenced by its high thermal motion parameters) seems to be responsible for the low-temperature behavior of the *q*-vector. The model used was based on the following *W*-matrices [9]:

$$W^1=\begin{matrix}1&0&0&0\\0&1&0&0\\0&0&1&0\\0&0&0&1\end{matrix},\quad W^2=\begin{matrix}1&0&0&0\\0&1&0&2\\0&0&1&0\\0&0&0&2\end{matrix},$$

$$W^3=\begin{matrix}1&0&0&0\\0&1&0&1\\0&0&1&0\\0&0&0&1\end{matrix},$$

Where all non-copper atoms belonging to the first composite part, Cu1 belonging to the second composite part, and Cu2 to the third. Using this model the structure was solved and refined, but it was evident that

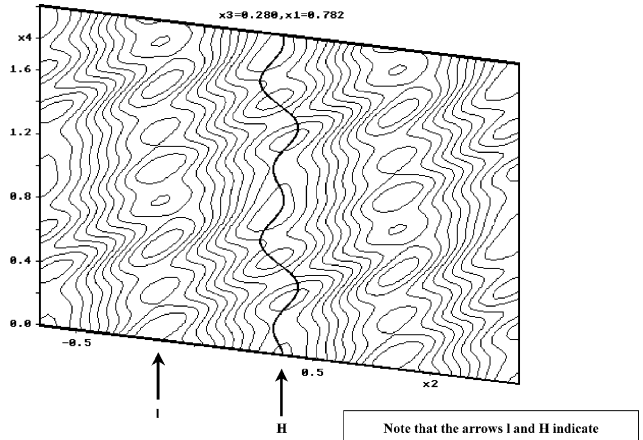

(a)

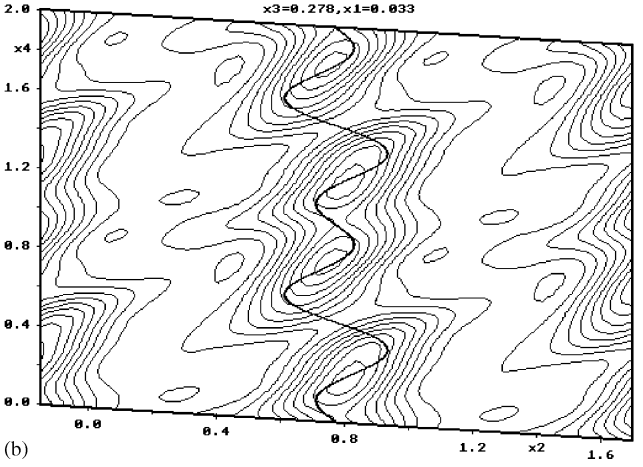

(b)

Fig. 3. Electron density map of Cu1 (a) and Cu2 (b). The maps are summation in the x_2-x_4 plane. Heavy lines indicate the model.

Table 1
Crystallographic, data collection and refinement parameters

Crystal parameters	
a	15.280(3)
b_1	3.616(1)
c	14.674(3)
α	90.0
β	101.95(2)
γ	90.0
q	0, 0.11, 0
b_2	$1/(\mathbf{b}_1^*+2\mathbf{q})= 2.964(1)$
b_3	$1/(\mathbf{b}_1^*+1\mathbf{q})= 3.257(1)$
Crystal system	Triclinic
Superspace group	$X1(\alpha\beta\gamma)$, Centering vectors 0000, 1/2 1/200, 001/2 1/2, 1/2 1/2 1/2 1/2
Measurement parameters	
Measuring device	STOE IPDS
Measuring temperature	Ambient
Radiation	Mo$K\alpha$
Wavelength	0.71073 Å
Absorption correction	Numerical from shape
Number of refls.	2458
Number of obs. refls.	988
Observation criterion	$I>3\sigma(F^2)$
μ	9.3 mm^{-1}
R_{int} obs/all	4.81/8.71
hklm limits	$-18<h<18;0<k<4;$ $-18<l<16;-2<m<2$
Refinement details	
All R_w, R_{w0}, R_{w1}, R_{w2}	6.1, 5.1, 15.2, 14.9
Obs R_w, R_{w0}, R_{w1}, R_{w2}	5.2, 5.0, 9.6, 7.2
Weighting scheme	$1/\{\sigma^2(F)+0.0001F^2\}$
Δ/esd	0.2
$\Delta\rho_{min}$, $\Delta\rho_{max}$	-5.1, 5.9 $eÅ^{-3}$
Number of parameters	308

Table 2
Atomic positions and thermal displacement parameters

Atom	x	y	z	U_{iso} or U_{eq}
First composite part, b=b1				
V1	0.1401(4)	−0.235(3)	0.1004(6)	0.0045(2)
V2	0.3627(4)	−0.234(3)	0.1019(6)	0.0045(2)
V3	0.7097(4)	−0.234(3)	0.4581(6)	0.0045(2)
V4	0.9218(4)	−0.235(3)	0.4490(6)	0.0045(2)
O1	0.035(1)	−0.240(8)	0.029(2)	0.0054(6)
O2	0.2242(9)	−0.230(6)	0.494(1)	0.0054(6)
O3	0.4083(8)	−0.246(5)	0.472(1)	0.0054(6)
O4	0.4574(9)	−0.226(6)	0.174(1)	0.0054(6)
O5	0.2823(9)	−0.227(6)	0.175(1)	0.0054(6)
O6	0.1140(9)	−0.210(6)	0.208(1)	0.0054(6)
O7	0.6155(9)	−0.232(6)	0.380(1)	0.0054(6)
O8	0.7865(4)	−0.228(3)	0.3795(7)	0.0054(6)
O9	0.9460(9)	−0.217(5)	0.348(1)	0.0054(6)
O10	0.8481(9)	−0.223(6)	0.063(1)	0.0054(6)
O11	0.6666(9)	−0.238(6)	0.077(1)	0.0054(6)
Second composite part, b=b2				
Cu1	0.7818(3)	0.361(3)	0.2795(4)	0.0345(14)
Third composite part, b=b3				
Cu2	0.0328(5)	0.776(4)	0.2781(7)	0.0403(15)

Anisotropic displacement parameters

Atom	$U11$	$U22$	$U33$	$U12$	$U13$	$U23$
Cu1	0.0132(8)	0.064(3)	0.025(2)	−0.001(1)	0.001(1)	−0.006(2)
Cu2	0.020(1)	0.083(4)	0.018(1)	−0.006(2)	0.0030(8)	0.009(2)

the behavior of the Cu positions is not fully resolved. While the failure in the X-ray measurement to detect the weak modulation at (1/2, ~0.16,0) will clearly leave some unresolved disorder in the structure, the difficulties in reaching a satisfactory refinement appeared more severe, and since the mirror plane of the monoclinic room temperature structure cannot be retained in a fully ordered model, the symmetry was reduced to triclinic in an attempt to ameliorate this. From W matrices it is clear that main reflections are given by the relations for reflections *hklm*:

m=0: main reflections of the first composite part (V_4O_{11}),

m=2k: main reflections of the second composite part (Cu1),

m=k: main reflections of the third composite part (Cu2).

All other reflections are true satellites, emanating from the interaction between the sub-lattices.

The final model uses second-order harmonics for the displacive modulation, corresponding to one harmonic wave from each of the two distinct modulation periodicities $\mathbf{q_1}$ and $2\mathbf{q_1}$, of all atoms as well as for the modulation of the thermal tensors of the Cu atoms. All non-copper atoms were treated as isotropic with the same value for all vanadium or all oxygen atoms. This may seem excessive, but since the major contribution to the scattering is the second-order satellites ($2\mathbf{q_1}$), it is necessary for a reasonable fit. In all, this yields 308 parameters to model the intensity of 2458 independent reflections, 988 with intensities $> 3\sigma(F^2)$. The final R_w-values were 6.1% for all reflections, and 5.2% for observed reflections. Only the Cu atoms show major displacive motions, and these are shown in Fig. 3. All data pertaining to the data collection are given in Table 1, atomic positions in Table 2, and magnitudes of harmonic modulations in Table 3.

3.2. Structure description

The determination of the $Cu_{2.33-x}V_4O_{11}$ modulated structure at low temperature allows us to describe it as a three parts composite structure. The different parts differ by their **b** cell parameter but have the same ac-plane. The first part corresponds to the $[V_4O_{11}]_n$ layers and is identical to the one determined previously in the average structure. VO_6 octahedra share edges to form a double zig-zag chain with the formula $[V_4O_{12}]_n$ developed along the **b**-axis. These double chains share corners along the **a**-axis to form the $[V_4O_{11}]_n$ layer developed in the ac-plane and stacked along the **c**-axis.

This stacking defines two kinds of tunnels, well described by the average structure, in which the copper ions are inserted. The occupancy of these tunnels by the copper ions is responsible for the two other parts of the composite structure.

Table 3
Coefficients of Fourier expansions of displacive modulations

Atom	cos$x$1 cos$x$2	Sin$x$1 Sin$x$2	cos$y$1 cos$y$2	sin$y$1 sin$y$2	cos$z$1 cos$z$2	sin$z$1 sin$z$2
V1	0.0043(5)	0.0021(4)	0.000(2)	−0.0227(6)	0.0019(7)	0.0017(5)
	0.0028(5)	0.0011(5)	0.000(2)	0.007(2)	0.0047(6)	0.0022(6)
V2	0.0068(4)	0.0024(5)	0.000(2)	0.004(2)	0.0038(6)	0.0032(6)
	0.0004(4)	−0.0003(5)	−0.004(2)	0.002(2)	0.0048(6)	0.0025(5)
V3	−0.0040(4)	−0.0021(5)	−0.003(2)	−0.002(2)	−0.0022(6)	−0.0031(7)
	0.0023(4)	0.0010(5)	0.004(2)	−0.003(2)	0.0079(5)	0.0042(6)
V4	−0.0035(5)	−0.0013(4)	−0.001(2)	0.012(2)	−0.0006(7)	−0.0008(6)
	0.0032(4)	0.0017(5)	0.003(2)	−0.005(2)	0.0067(6)	0.0035(6)
O1	0.007(1)	0.000(2)	−0.013(5)	0.00(1)	0.005(1)	−0.001(3)
	0.005(1)	−0.001(2)	0.000(7)	0.003(7)	0.009(2)	0.001(2)
O2	−0.006(2)	−0.002(2)	−0.010(9)	0.004(9)	−0.004(2)	−0.003(3)
	0.002(2)	0.002(2)	0.006(8)	−0.001(8)	0.005(2)	0.005(2)
O3	−0.006(2)	−0.001(2)	0.014(9)	−0.008(9)	−0.002(2)	−0.004(2)
	0.005(2)	−0.000(2)	−0.007(8)	−0.005(8)	0.010(2)	−0.000(2)
O4	0.006(2)	0.0020(2)	0.003(9)	0.022(8)	0.002(2)	0.002(2)
	−0.000(2)	0.002(2)	0.004(7)	0.010(8)	0.002(2)	0.002(2)
O5	0.007(2)	0.000(2)	−0.002(9)	−0.017(8)	0.004(2)	−0.003(2)
	0.0020(1)	0.002(1)	−0.040(7)	0.059(6)	0.005(2)	0.000(1)
O6	0.007(2)	0.007(1)	0.012(9)	0.003(8)	0.003(2)	0.003(2)
	0.001(2)	0.000(2)	−0.010(8)	0.026(7)	0.005(2)	−0.004(2)
O7	−0.006(2)	−0.002(2)	0.000(9)	−0.015(8)	−0.004(2)	−0.000(2)
	0.003(2)	0.003(2)	0.012(7)	0.002(7)	0.008(2)	0.004(2)
O8	−0.005(1)	0.004(1)	−0.005(5)	0.014(6)	−0.001(1)	0.009(1)
	−0.001(1)	0.001(1)	0.003(6)	−0.014(6)	−0.001(1)	0.003(1)
O9	−0.003(2)	−0.004(2)	0.019(8)	−0.012(9)	0.001(2)	−0.002(2)
	0.002(2)	0.005(2)	0.006(7)	0.002(7)	0.008(2)	0.006(2)
O10	0.003(2)	−0.001(2)	−0.004(9)	0.010(9)	−0.001(2)	−0.002(2)
	0.002(2)	0.002(2)	−0.012(8)	0.000(8)	0.004(2)	0.006(2)
O11	0.003(2)	−0.000(2)	0.016(9)	0.010(9)	0.001(2)	0.002(2)
	0.005(2)	0.002(2)	0.000(8)	−0.001(8)	0.0026(6)	0.002(2)
Cu1	−0.0020(3)	−0.0009(4)	−0.017(3)	0.038(3)	0.0208(4)	0.0186(5)
	0.0002(5)	0.0004(5)	0.034(4)	−0.035(3)	−0.0064(5)	−0.0064(6)
Cu2	0.0034(3)	0.0007(2)	−0.004(2)	0.072(2)	−0.0041(5)	−0.0007(3)
	−0.0011(5)	0.0004(5)	0.004(4)	−0.107(3)	0.0026(6)	0.0044(6)
Atom	U11cos1 U12cos1 U11cos2 U12cos2	U11sin1 U12sin1 U11sin2 U12sin2	U22cos1 U13cos1 U22cos2 U13cos2	U22sin1 U13sin1 U22sin2 U13sin2	U33cos1 U23cos1 U33cos2 U23cos2	U33sin1 U23sin1 U33sin2 U23sin2
Cu1	0.003(2)	0.005(2)	0.037(5)	−0.010(6)	0.032(4)	0.000(4)
	−0.003(3)	−0.003(3)	−0.005(3)	−0.002(2)	−0.034(4)	0.058(4)
	−0.011(4)	0.005(2)	−0.054(7)	−0.047(8)	−0.021(6)	−0.006(2)
	0.020(4)	−0.008(2)	−0.011(4)	0.001(2)	−0.004(5)	0.024(3)
Cu2	−0.015(2)	−0.020(3)	−0.020(8)	0.005(8)	−0.004(4)	0.024(4)
	0.005(3)	0.021(4)	0.013(2)	0.002(3)	−0.007(4)	−0.030(5)
	−0.001(3)	0.006(3)	−0.045(8)	0.054(9)	0.001(4)	−0.002(4)
	0.027(4)	−0.051(4)	−0.011(3)	0.002(3)	0.052(5)	−0.013(5)

The first one (Cu1) presents a unit-cell repeat of $b = 2.964$ Å. Fig. 4a represents the drawing of Cu1 surrounding using a 8^*b periodic approximation. One can note that it forms a kind of chain of successively linear and triangular surrounding in agreement with the different sites used to describe the average structure. Longer Cu–O distances can also be taken into account driving to consider the surroundings to be successively distorted square planar (instead of linear) and tetrahedral (instead of triangular). These longer distances correspond to the attraction of copper ions on the oxygen atoms O6 and O9 ending the $[V_4O_{12}]_n$ double chains and explain its puckering.

The second one (Cu2) presents a unit-cell repeat of $b = 3.257$ Å. It corresponds to the tetrahedraly surrounded site observed in the average structure. Despite the fact that it was possible to describe it as a well-ordered site, the thermal motion was found to be very high in the average structure description. Both the TEM and X-ray studies of the incommensurate structure

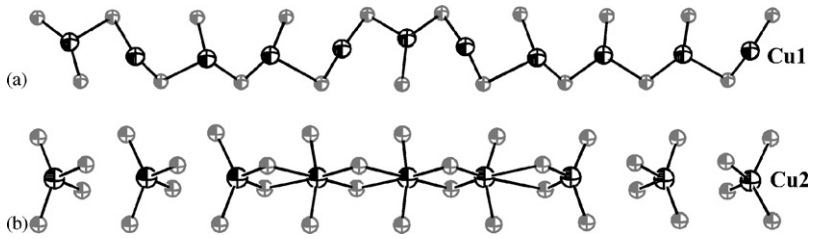

Fig. 4. Periodic approximation (8^*b) of the structure for Cu1 (a) and Cu2 (b).

support the conclusion that in fact this copper site is the most disordered at room temperature and that it appears to condense out at low temperature. Fig. 4b represents the drawing of Cu2 surrounding, here again using the periodic 8^*b approximation. It can be described as a chain built up with a smooth evolution from tetrahedral to octahedral surrounding evidenced by the continuous variation of the Cu–O distances along the modulation.

The use of such a composite structure allows then to describe each of the two copper sites by only one and fully occupied copper crystallographic site. This appears to be more reasonable than the description made by Kato et al. [3], which implies the use of two modulated and partially occupied sites to describe the first tunnel (Cu1) and up to six modulated and partially occupied (sometime very low amounts) positions to describe the second one (Cu2).

3.3. Composition and copper valence state

$Cu_{2.33}V_4O_{11}$ appears to be well described by the use of a three parts composite structure. The first one corresponding to the $[V_4O_{11}]_n$ layers is close to the one determined in the average structure while the two others, used for the copper ions description, differs by the **b** cell unit repeat. Then copper content can be derived from the mismatch between the **b** cell repeat of the different parts. Considering the second part (Cu1 in the linear and triangular surroundings) the **b** cell repeat is equal to $1/(\mathbf{b}_1^* + 2\mathbf{q})$ where $\mathbf{b_1}$ is the cell repeat of the first part ($[V_4O_{11}]_n$ layers) id est close to 2.964 Å; This means considering the size of the cell defined by the $[V_4O_{11}]_n$ layer and one fully occupied copper site in the second part that leads to a total Cu1 amount equal to $\mathbf{b_1}/\mathbf{b_2} = 1.220$ per V_4O_{11}unit. Considering the third part, its unit cell repeat is $b_3 = 1/(\mathbf{b}_1^* + \mathbf{q}) = 3.257$ Å. Here again, only one copper site is used to describe this tunnel occupancy, and the refinement clearly shows that it is fully occupied. This leads to a Cu2 amount equal to $\mathbf{b_1}/\mathbf{b_3} = 1.110$. Then the global copper content is estimated as 2.33 per V_4O_{11} unit which corresponds perfectly to the one determined in the average structure but without any kind of partially occupied crystallographic position. Here again, this implies that the maximal copper content

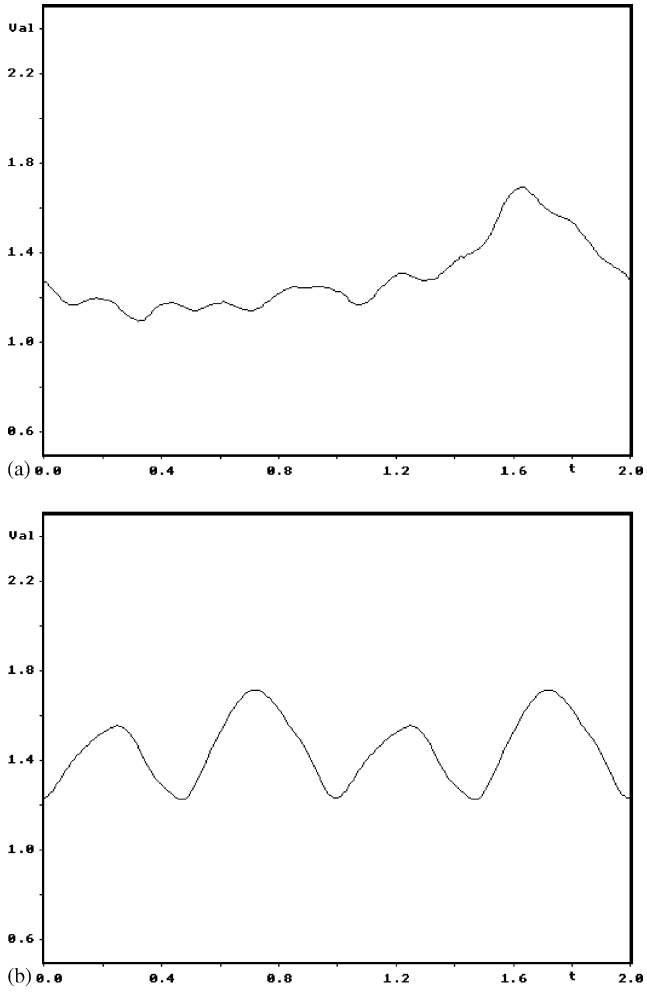

Fig. 5. Bond valence sums for the Cu1 (a) and Cu2 (b) ions.

of this phase is reached for $x = 0$ in the formula $Cu_{2.33-x}V_4O_{11}$.

The last point concerns the difficulty encountered for the determination of both copper and vanadium valence states. As previously reported [10], it appears both on magnetic and electric properties as well as chemical routes used that there is an equilibrium between $+1/+2$ valence states for the copper and $+4/+5$ ones for the vanadium driving to the formula: $Cu^{+1}_{2.33-a}Cu^{+2}_{a}V^{+5}_{4-b}V^{+4}_{b}O_{11}$.

In this formula, to insure the electroneutrality of the compound, **a** can range from 0 to 2.33 and **b** from 0.33 to 2.66; this latter values being of course interdependent showing the wide range of possible solutions. XPS experiments on different samples have revealed that the Cu^{+}/Cu^{2+} ratio is equal to 1.11 while the overlap of V characteristic bands cannot be allowed to conclude about the V^{4+}/V^{5+} ratio. In the mean time, electronic band structure calculation based on the average structure have shown that +2 valence state can be assigned to the copper in tetrahedral surrounding and +1 to those with the mixed linear and triangular one [10] which correspond, respectively, to the third and second part of the composite structure. Using the crystallographic data of the average structure, leads to a calculated ratio $Cu^{+}/Cu^{2+} = 1.33$ slightly higher than the experimental one determined from XPS experiments, implying the existence of remaining doubts about the balance between V and Cu valence states.

Using the data issued from the composite structure, we mentioned above that the copper content per V_4O_{11} unit is equal to 1.22 for Cu1 and to 1.11 for Cu2. Fig. 5 shows bond valence sums calculated for copper ions [11,12]. The results are in perfect agreement with electronic structure calculations made on the basis of the average structure. Then, keeping the hypothesis that the Cu^{+2} is assigned to Cu2 and Cu^{+1} is assigned to Cu1 that leads to a Cu^{+}/Cu^{2+} ratio equal to 1.10 in perfect agreement with the experimental one. The amount of V^{4+} and V^{5+} in this structure can then be calculated according to the formula $Cu^{+1}_{1.22}Cu^{+2}_{1.11}V^{+5}_{2.56}V^{+4}_{1.44}O_{11}$.

4. Conclusion

The refinement of $Cu_{2.33}V_4O_{11}$ incommensurate structure on the basis of XRD experiments allows us to describe it as a three parts composite structure each of them different by the b cell unit repeat while keeping the same ac-plane. The $[V_4O_{11}]_n$ layers are related to the first substructure and each of the two copper sites to the second and third ones. This allows us to describe the entire structure using only two different copper sites each of them being fully occupied. Using such results, the composition can be calculated from the mismatch of the different b-repeat driving to $Cu_{2.33}V_4O_{11}$ in agreement with previous results. Moreover, bond valence sums agree with electronic structure calculations to attribute to each of the copper sites the proper valence state. Combined with respective occupation, the ratio $Cu^{+}/Cu^{2+} = 1.10$ is obtained in perfect agreement with the results issued from XPS experiments ($Cu^{+}/Cu^{2+} = 1.11$).

Acknowledgments

We wish to thank V. Petricek for helpful discussions and improvement of the JANA program.

References

[1] J. Galy, D. Lavaud, A. Casalot, P. Hagenmuller, J. Solid State Chem. 2 (1970) 531.
[2] Y. Saito, M. Onoda, H. Nagasawa, J. Phys. Soc. Jpn. 61 (1992) 3865.
[3] K. Kato, K. Kosuda, Y. Saito, H. Nagasawa, Z. Kristallogr. 211 (1996) 522.
[4] P. Rozier, C. Satto, J. Galy, Solid State Sci. 2 (2000) 595.
[5] R.L. Withers, P. Rozier, Z. Kristallogr. 215 (2000) 688.
[6] X-Red: STOE Data Reduction Program, STOE & Cie GmbH, Darmstadt, Germany, 1996.
[7] Jana2000, V. Petricek, Crystallographic Computing Program, Institute of Physics, Academy of Sciences of the Czech Republic, Prague, Czech Republic, 2000.
[8] Space: STOE Data program, STOE & Cie GmbH, Darmstadt, Germany, 1996.
[9] S. Van Smaalen, Phys. Rev. B 43 (1991) 11330.
[10] P. Rozier, J. Galy, G. Chelkowska, H.J. Koo, M.H. Whangbo, J. Solid State Chem. 166 (2002) 382.
[11] I.D. Brown, D. Altermatt, Acta Crystallogr B 41 (1985) 244.
[12] N.E. Brese, O'Keeffe, Acta Crystallogr. B 47 (2) (1991) 192.